

Ni^{II}, Pd^{II} and Pt^{IV} complexes of Heterocyclic ligands derived from 1,3,4Thiadiazole and Pentaerythritol tetra bromide, Synthesis, characterization and biological Study

Maha R. Hashim^{1*}, MahaS. Hussein^{1*}, and Ashour H. Dawood²

¹Samarra' University, Education College, Department of chemistry, Iraq

²Al-Mustansiriyah University, Pharmacy College, Department of Pharmaceutical chemistry, Iraq

Abstract : The synthesis was carried out of type ligands from 5-amino- 1,3,4-thiadiazole-2-thiol with pentaerythritoltetrabromide and 1, 3, 4-Thiadiazole-2, 5-dithiol with pentaerythritoltetrabromide through the condensation reaction, since the CS₂ was reacted with thiosemicarbazide to form the main precursor1. The ligand was obtained by the addition to precursor1 to pentaerythritoltetrabromide in 4:1 ratio. While the other ligand obtained via the reaction of hydrazine hydrate with two equivalent of (CS₂) to form the precursor2, the pentaerythritoltetrabromide treated with precursor2 resulted ligand2. The prepared ligands were characterised by ¹H- ¹³C NMR, FTIR, UV-Vis and GC spectroscopies, as well as the physical properties. The Ni⁺², Pd⁺² and Pt⁺⁴ complexes of these ligands were prepared through the reaction one equivalent of ligand to two equivalent of metal ions. The binuclear complexes were obtained and characterised by FTIR and UV-Vis spectroscopies, conductivity, magnetic susceptibility and melting point were measured. The biological activity of the prepared ligands and their complexes carried out with *staphylococcus aureus* and *E-coli* bacteria. The results showed the (15ppm) concentration of Pt⁺⁴ and Ni⁺² of L² are the best one of them. From the spectral studies the suggested geometry of complexes as octahedral geometry for Ni⁺² and Pt⁺⁴ ions, while square planer of Pd⁺² ion.

Keywords : Thiadiazole derivatives, biological activity, Nickel Palladium Platinum Complexes.

Introduction

Thiadiazole is a 5-membered ring system containing hydrogen-binding domain, sulphur atom, and two-electron donor nitrogen system (–N=C–S) that exhibit a wide variety of biological activity¹. There are several isomers of thiadiazole, that is, 1, 2, 3-thiadiazole, 1, 2, 5-thiadiazole, 1, 2, 4-thiadiazole and 1, 3, 4-thiadiazole. 1,3,4-Thiadiazole was first described in 1882 by Fischer⁽²⁾ and further developed by Bush and his coworkers, but true nature of the ring system was demonstrated first in 1956 by Goerdler et al³. 1,3,4-Thiadiazole have become very important compounds in agriculture, industrial, medicine and many fields of technology⁴. It used in several applications as organic compound or as a ligand in inorganic complexes, the best method to produce it was reported by Jumath Salimon and co-workers⁵. Among the various clinical applications, 1, 3, 4-Thiadiazole have a considerable active role as anti-inflammatory⁶, anti-tumor drugs⁷, Antimicrobial and Antioxidant⁸, anti-viral⁹. The development from the sixties demonstrate that the 1,3,4-thiadiazole and their derivatives have received much interest in the field of Agriculture, Medicine and Industry¹⁰. This is primarily due to large number of uses of 1,3,4-thiadiazoles in the most diverse areas, for examples, dyestuffs industry,

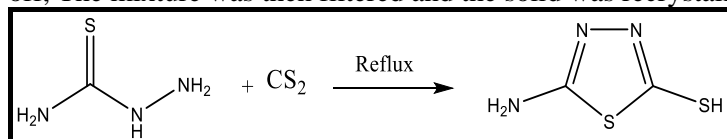
photography and corrosion inhibitors¹¹. General applications of thiadiazole derivatives are as vast as they are diverse and are not extensively encompassed in the scope of this review. In this study were synthesized a heterocyclic ligands contain 1,3,4-thiadiazole ring and their complexes with Ni(II), Pd(II) and Pt(IV) and investigated. Through synthesized two of thiadiazole derivatives¹² while was obtained the ligands from treated the derivatives with pentaerythritoltetrabromide in 4:1 ratio. The FT-IR, UV-Vis spectroscopies, Molar Conductivity and Magnetic susceptibility of the study was shown that the structure of complexes Ni^{II}, Pt^{IV} octahedral and the Pd^{II} complexes was square-planar. And evaluation of their *antimicrobial* activities compounds and 1,3,4-thiadiazoles¹³ were screened for their *antibacterial* activity against *S.aureus* (gram-positive) and *E. coli* (gram-negative) bacteria.

2-Experimental part:

All chemical materials and reagents have been used without purification, so they were supplied from Aldrich, Merck, B.D.H and G.C.C companies. IR spectra were recorded as KBr discs using a Shimadzu 8400s FTIR spectrophotometer in range (4000-400) cm⁻¹. Electronic spectra of the prepared compounds were measured in the region (200-900) nm for (1*10⁻³M) solution in DMSO-d⁶ at 25 °C using Shimadzu 1650 spectrophotometer, with 1.000 ± 0.001 cm matched quartz cell. ¹H, ¹³C- NMR were acquired with Bruker Ultra Shield 400MHz spectrometer in DMSO-d⁶. Elemental microanalysis was performed on a (C.H.N.S) analyser from EuroEA elemental analyser, the Magnetic Susceptibility was carried out from MSB-Auto. The Molar Conductivity of the complexes was recorded at 25°C for (1*10⁻³ M). Solution of the sample in DMSO-d⁶ using a PW9526 digital conductivity meter. The gas chromatography spectra were recorded at GC Shimadzu, GC Chromatograph 2010.

2:1-Preparation 5-amino- 1,3,4-thiadiazole-2-thiol(Compound1)

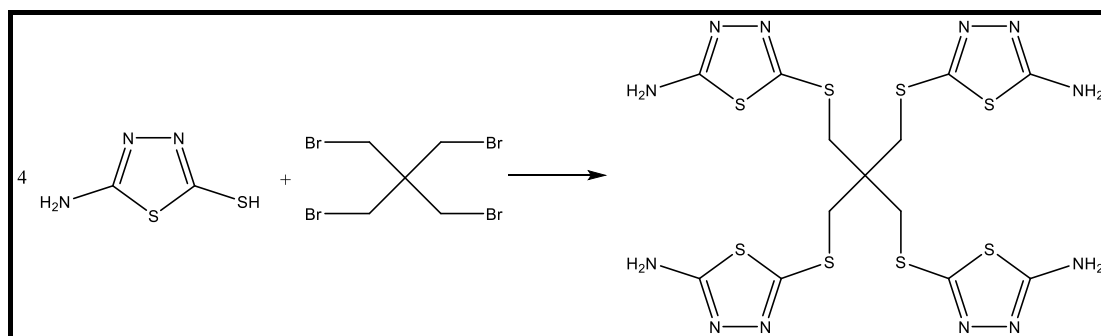
Carbendisulfide CS₂ (0.7mL) was added to the stirred solution from Thiosemicarbazide (1g, 10.97mmol.) in (20mL) of pyridine, the mixture was refluxed at (70°C) for (2.5 h.). Then the excess solvent was then distilled off, The mixture was then filtered and the solid was recrystallized from diethylether¹⁴, **Scheme (1)**.



Scheme (1) Synthesis route of compound 1

2:2-Preparation [5,5'-((2,2-bis(((5-amino-1,3,4-thiadiazol-2-yl)thio)methyl)propane-1,3-diyl)bis(sulfaneyl))bis(1,3,4-thiadiazol-2-amine)]

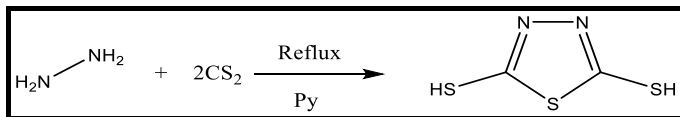
pentaerythritol tetrabromide (0.1g ,0.257mmol.) and (0.3g, 2.17mmol.) from potassium carbonate K₂CO₃ dissolved in (20mL) ethanol the PH adjusted to 8.5-9.0. This solution was added slowly to the 5-amino-1,3,4-thiadiazole-2-thiol (0.137g, 1.028mmol.) dissolved in (20mL) ethanol. The mixture was refluxed at (80°C) for (2h.). The mixture then cooled at room temperature, filtered, washed twice with diethylether, recrystallized with methanol and benzene, dried to obtained ligand [L¹], **Scheme(2)**.



Scheme (2) Synthesis route of Ligand L¹

2:3-Preparation of 1,3,4-Thiadiazole-2,5-dithiol (Compound2)

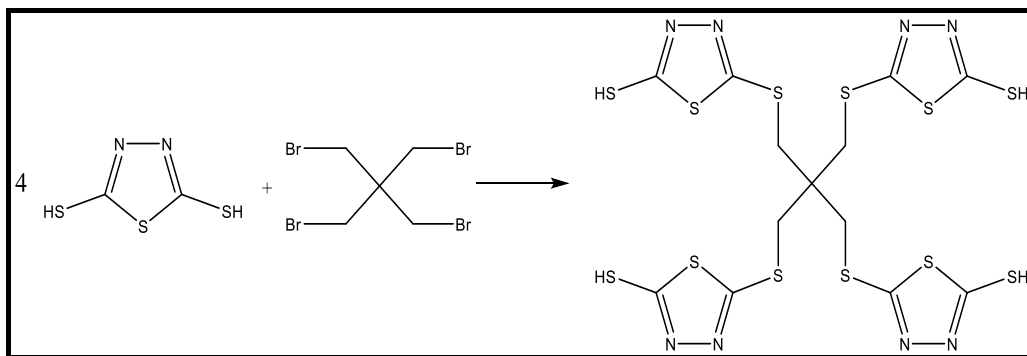
Mixtures of (98%) hydrazine hydrate (1g, 31.2mmol.) and carbon disulfide (2mL) in ethanol media was refluxed for (2 h.) at (70°C). Then the excess solvent was then distilled off, The mixture was then filtered and the solid was recrystallized from diethylether⁽²⁾, **Scheme (3)**.



Scheme (3) Synthesis rout of compound 2

2:4-Preparation of 5,5'-((2,2-bis(((5-mercapto-1,3,4-thiadiazol-2-yl)thio)methyl)propane-1,3-diyl)bis(sulfanediyl))bis(1,3,4-thiadiazole-2-thiol)

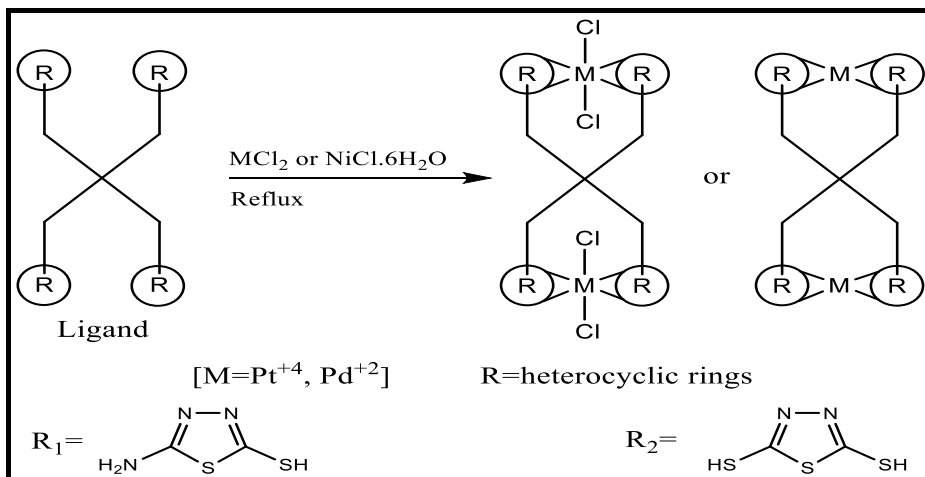
The solutions of (0.1g ,0.257mmol.) from pentaerythritol tetrabromide and (0.3g, 2.17mmol.) of potassium carbonate K_2CO_3 in (20mL) of ethanol, with adjusted PH rang between (8.5-9.0) were added slowly to solution of (0.145g,1.024mmol.) from (1,3,4-thiadiazole-2,5dithiol) in (20mL) ethanol, the mixture refluxed at (80°C) for (2h.). The mixture cooled at room temperature, filtered, washed twice times with diehylether, recrystallized with methanol and benzene, dried to obtained ligand $[L^2]$, **Scheme(4)**.



Scheme (4) Synthesis rout of Ligand L^2

2:5-Preparation of the Ligand's Complexes

Methanolic solution of the suitable metal salts [Palladium (II) chloride, Platinum (IV) Chloride and Nickel(II) chloride hexahydrate] was added to methanolic solution of compounds (1) and (2) respectively in 2:1 (metal:ligand) molar ratio and refluxed for (1.5h.)¹⁵. crystalline colored precipitates were formed at room temperature. The resulting solids were washed by diethyl ether and left to dried.



Scheme (5) the complexes structure of Ni^{II} , Pd^{II} and Pt^{IV}

2:5:1-L¹ complexes with Ni^{II}, Pd^{II}, Pt^{IV}

Methanolic solution (5mL) of the selected metal ion salts (0.19g, 0.799mmol.), (0.14g, 0.789mmol.), (0.28g, 0.831mmol.) of NiCl₂.6H₂O, PdCl₂ and PtCl₂ respectively were added as drop wise to methanolic solution (20mL) (0.25g, 0.419mmol.) from L². Refluxed the mixture for (1.5h.) at (70⁰C). When complete the reaction cooled the product at room temperature. Filtered the precipitate washed two times with diethyl ether. The physical properties of these complexes are listed in **table (3)**.

2:5:2-L² complexes with Ni^{II}, Pd^{II}, Pt^{IV}

Methanolic solution (5mL) of the selected metal ion salts (0.17g, 0.715mmol.), (0.13g, 0.733mmol.), (0.2g, 0.593mmol.) of NiCl₂.6H₂O, PdCl₂ and PtCl₂ respectively were added as drop wise to methanolic solution (20mL) (0.25g, 0.371mmol.) from L². Refluxed the mixture for (1.5h.) at (70⁰C). When complete the reaction cooled the product at room temperature. Filtered the precipitate washed two times with diethyl ether. The physical properties of these complexes are listed in **table (3)**.

2:6-Biological activity of the ligands and its metal complexes

The biological activity of the ligands (L) and its complexes was examined against two types of bacteria, *E-coli* as grame-negative bacteria and *Staphylococcus aureus* as grame-positive bacteria were cultivated in nutrient agar medium all samples were freshly prepared by dissolving them in DMSO to obtain a final concentration of (5ppm), (10ppm) and (15ppm). The antibacterial test was performed according to disc diffusion method⁽¹⁶⁾. Which involves the exposure of micro-organism on agar plate. The plates were incubated for 24 hours at 37 C⁰, the zone of inhibition of bacterial growth around the disc was observed, the results are shown in **table (4)**.

3-Results and discussion

The purity of the compounds was checked by elemental analysis and constancy of melting points **Table (1)**. Then Ni⁺², Pd⁺² and Pt⁺⁴ metal ions added to form the binuclear complexes in 2:1 ratio **M:L**. the solubility of compounds was recorded in deferent solvents **Table(2)**.

Table (1) Elemental analysis and physical properties of prepared compounds

NO.	Color	Formula	Yield %	m. p (C)	Elemental analysis calc.(found)			
					C%	H%	N%	S%
1	pale yellow	C ₂ H ₃ N ₃ S ₂	71	162-164	-	-	-	-
2	Purple fine powder	C ₁₃ H ₁₆ N ₁₂ S ₈	58	263-265	26.16 (26.08)	2.70 (2.77)	28.16 (28.19)	42.98 (42.87)
3	Yellow	C ₂ H ₂ N ₂ S ₃	39	147-149	15.99 (15.98)	1.34 (1.35)	18.65 (18.64)	64.03 (64.04)
4	Pale yellow crystals	C ₁₃ H ₁₂ N ₈ S ₁₂	26	276-278	23.48 (23.40)	1.28 (1.89)	16.85 (16.91)	57.86 (57.80)

Table (2) Solubility the ligands and their complexes in different solvents

(+) Soluble

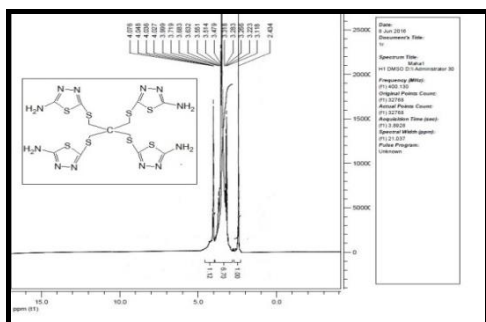
(–) Insoluble

(÷) Sparingly

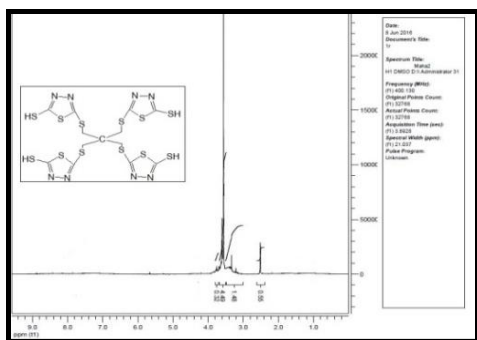
Compound	DMSO	DMF	BENZENE	H ₂ O	Ethanol
Ligand1	+	+	–	+	+
Ligand2	+	+	–	÷	+
Ni ^{II} ,L ¹	+	+	–	–	÷
Pd ^{II} ,L ¹	+	+	–	÷	–
Pt ^{IV} ,L ¹	+	+	–	–	–
Ni ^{II} ,L ²	+	+	–	–	÷
Pd ^{II} ,L ²	+	+	–	–	÷
Pt ^{IV} ,L ²	+	+	–	÷	–

3:1- ¹H-NMR Spectra**3:1:1-¹H-NMR spectrum for the ligand1 [L¹]**

The ¹H NMR spectrum of [L¹] **Fig.(1)** in DMSO-d₆ displays the signal at (δ = 4.04 ppm, 8H) due to the protons for methyl groups(CH₂), the chemical shifts at (δ = 3.5ppm, 8H)attributed to the protons for amine groups (NH₂)¹⁷.

**Figure (1) ¹H-NMR spectrum of ligand1****3:1:2-¹H-NMR spectrum for the ligand2 [L²]**

The ¹H NMR spectrum of [L²] **Fig.(2)** in DMSO-d₆ exhibitsthe signal at (δ=4.1ppm,4H)assigned to the protons for thiol groups (SH) at Thiadiazole ring, the chemical shifts at (δ = 3.5ppm, 8H)referred tothe protons for amine groups (NH₂)¹⁷.

**Figure (2) ¹H-NMR spectrum of ligand 2**

3:2- ^{13}C -NMR Spectra

3:2:1- ^{13}C -NMR spectrum for the ligand1 [L^1]

The ^{13}C -NMR spectrum of [L^1] Fig.(3) in DMSO-d_6 shows the signal at ($\delta = 166.9\text{ppm}$) attributed to the carbon atoms C^a of carbon-nitrogen double bond($\text{C}=\text{N}$), the signals at ($\delta = 159.6\text{ppm}$) due to the carbon atoms C^b of carbon-nitrogen double bond, while the carbon atoms C^c appeared signal at ($\delta = 67.3\text{ppm}$), the carbon atoms C^d of carbon-sulfur single bond shows the signals at ($\delta = 28.8\text{ppm}$)⁽¹⁷⁾.

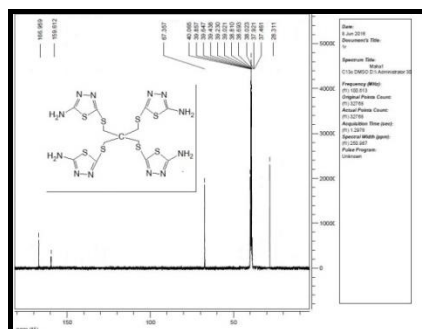


Figure (3) ^{13}C -NMR spectrum of ligand 1

3:2:2- ^{13}C -NMR spectrum for the ligand2 [L^2]

The ^{13}C -NMR spectrum of [L^2] Fig.(4) in DMSO-d_6 displays the signal at ($\delta = 166.9\text{ppm}$) referred to the carbon atoms C^a of carbon-nitrogen double bond($\text{C}=\text{N}$), the signals at ($\delta = 160.2\text{ppm}$) assigned to the carbon atoms C^b of carbon-nitrogen double bond, while the carbon atoms C^c appeared signal at ($\delta = 67.3\text{ppm}$) due to carbon-protons single bond, the carbon atoms C^d of carbon-sulfur single bond shows the signals at ($\delta = 39.2\text{ppm}$)⁽¹⁷⁾.

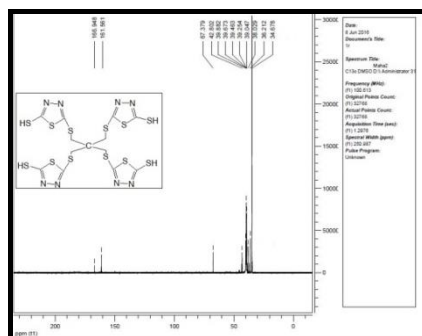


Figure (4) ^{13}C -NMR spectrum of ligand2

3:3-FT-IR Spectra of the precursors, ligands and complexes

3:3:1-FT-IR Spectrum of com.1

IR spectrum of 5-amino- 1,3,4-thiadiazole-2-thiol **Fig.(5)** exhibits bands at ($3338\text{--}3251\text{cm}^{-1}$) assigned to sym. and asym. Stretching of $\nu(\text{N-H})$ amine group ($-\text{NH}_2$). The weak characterized band at (2769cm^{-1}) attributed to the stretching of $\nu(\text{N-H})$ of thiol group (SH). While the band at (1606cm^{-1}) referred to the stretching of $\nu(\text{C}=\text{N})$ for thiadiazole ring. The bands at (1254cm^{-1}) and (1059cm^{-1}) assigned to stretching of $\nu(\text{N-N})$ and $\nu(\text{C-S})$ respectively^{18, 19}.

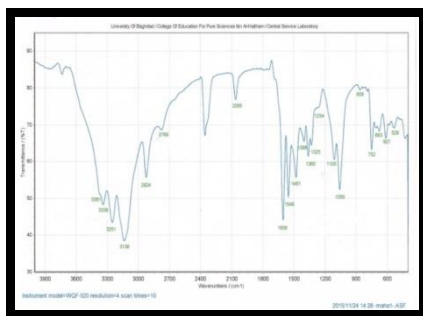


Figure (5) FT-IR spectrum of the compound 1

3:3:2-FT-IR Spectrum of com.2

IR spectrum of 2,5-dithiol 1,3,4-thiadiazole **Fig.(6)** displays band at (2576cm^{-1}) due to stretching $\nu(\text{S-H})$ of thiol group. While the band at (1568 cm^{-1}) characterize of thiadiazole ring of $\nu(\text{C=N})$ stretching. The bands at (1279 cm^{-1}) can be attributed to stretching of $\nu(\text{N-N})$. The band at (1047cm^{-1}) referred to $\nu(\text{C-S})$ of thiadiazole^{18, 19}.

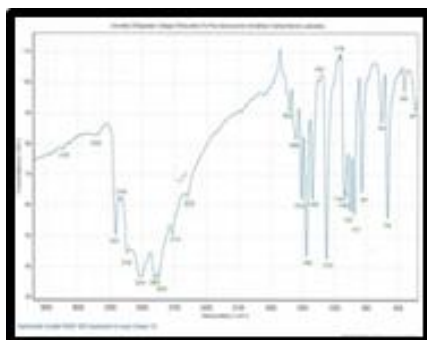
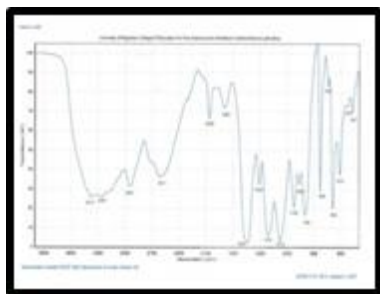


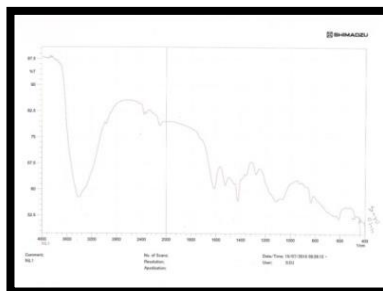
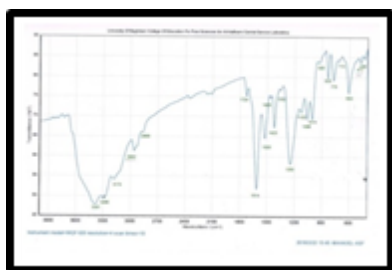
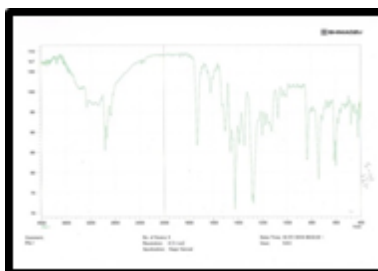
Figure (6) FT-IR spectrum of the compound 2

3:3:3-FT-IR Spectrum of ligand1

IR spectrum of Ligand1 **Fig.(7)** Shows new bands at ($3373\text{-}3255\text{cm}^{-1}$) assigned to sym. and asym. Stretching of $\nu(\text{N-H})$ amine group ($-\text{NH}_2$). The band at (2947 cm^{-1}) can be attributed to Stretching of $\nu(\text{C-H})$ aliphatic (CH_2) while the band at (1410 cm^{-1}) can be referred to bending of $\nu(\text{C-H})$ aliphatic (CH_2). The characterize band at (1633cm^{-1}) due to $\nu(\text{C=N})$ stretching of thiadiazole ring. The bands at (1063cm^{-1}), (999cm^{-1}) due to stretching of $\nu(\text{N-N})$, $\nu(\text{C-S})$ Thiadiazole ring respectively. While IR spectra for complexes **Fig.(9)(10)(11)** respectively for (Ni^{+2}) (Pd^{+2}) (Pt^{+4}) ions displays bands at (440cm^{-1}), (436cm^{-1}), (431cm^{-1}) respectively attributed to (M-S) to the coordination bonding between the ligand and metal ion^{18, 19}.



"Figure (7) FT-IR spectrum of the ligand 1"

" Figure (9) FT-IR spectrum of the ligand1with Ni^{II}"Figure (10) FT-IR spectrum of the ligand1with Pd^{II}Figure (11) FT-IR spectrum of the ligand1with Pt^{IV}

3:3:4-FT-IR Spectrum of ligand2

IR spectrum of Ligand2 **Fig. (8)** Exhibits band at (2954cm⁻¹) can be attributed to Stretching of ν(C-H) aliphatic (CH₂) while the band at (1410 cm⁻¹) due to bending of ν(C-H) aliphatic (CH₂). The band at (2621cm⁻¹) referred to Stretching of ν(S-H) of thiol group (SH), The bands at (1633cm⁻¹), (1038cm⁻¹), (1003cm⁻¹) assigned to stretching of ν(C=N), ν(N-N), ν(C-S) of thiadiazole ring respectively. While IR spectra for complexes **Fig.(12)(13)(14)** respectively for (Ni⁺²) (Pd⁺²) (Pt⁺⁴) ions shows bands at (425cm⁻¹), (444cm⁻¹), (429cm⁻¹) respectively attributed to (M-S) to the coordination bonding between the ligand and metal ion^{18,19}.

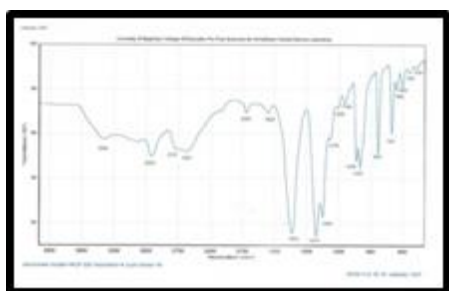
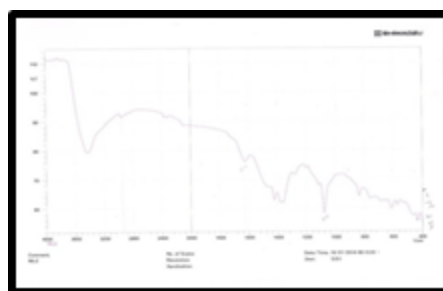


Figure (8)FT-IR spectrum of the ligand 2

"Figure (12)FT-IR spectrum of the ligand2with Ni^{II}

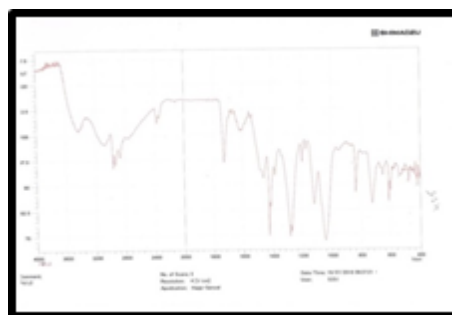
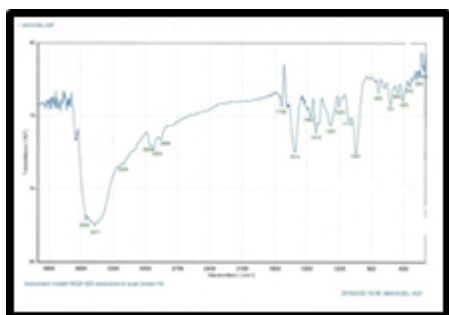


Figure (13) FT-IR spectrum of the ligand2 with Pd^{II} Figure (14) FT-IR spectrum of the ligand2 with Pt^{IV}

3:4-UV-Vis Spectra

3:4:1-UV-Vis spectra of (L^1) and their Complexes

The (UV-Vis) spectrum of [L^1] **Fig.(15)** exhibits a broad absorption peak between (272- 308 nm) ($36764 - 32467 \text{ cm}^{-1}$) ($E_{\text{max}} = 353\text{-}441 \text{ Lcm}^{-1}\text{mol}^{-1}$) assigned to ($\pi \rightarrow \pi^*$) transitions, The ($n \rightarrow \pi^*$) not appear clearly due to the broadness of peak of ($\pi \rightarrow \pi^*$). The (UV-Vis) spectra for L^1 complexes with Ni^{II} , Pd^{II} , Pt^{IV} ions **Fig.(16)(17)(18)** respectively displays the peaks at (330 nm) (30303 cm^{-1}) ($E_{\text{max}} = 210 \text{ Lcm}^{-1}\text{mol}^{-1}$), (318 nm) (31446 cm^{-1}) ($E_{\text{max}} = 732 \text{ Lcm}^{-1}\text{mol}^{-1}$) and (310 nm) (32258 cm^{-1}) ($1368 \text{ Lcm}^{-1}\text{mol}^{-1}$) for Ni^{II} , Pd^{II} , Pt^{IV} attributed to the ligand field and charge transfer. The Ni complex shows the peaks at (718 nm) (13927 cm^{-1}) ($E_{\text{max}} = 232 \text{ Lcm}^{-1}\text{mol}^{-1}$) and (600 nm) (16666 cm^{-1}) ($E_{\text{max}} = 224 \text{ Lcm}^{-1}\text{mol}^{-1}$) due to the d-d transition type ($^3\text{A}_{2g} \rightarrow ^3\text{T}_{1g}$) ($^3\text{A}_{2g} \rightarrow ^3\text{T}_{2g}$), and the Pt^{IV} complex shows the peaks at (522 nm) (19157 cm^{-1}) ($E_{\text{max}} = 68 \text{ Lcm}^{-1}\text{mol}^{-1}$) and (498 nm) (20080 cm^{-1}) ($51 \text{ Lcm}^{-1}\text{mol}^{-1}$) assigned to the d-d transition type ($^1\text{A}_{1g} \rightarrow ^1\text{T}_{1g}$) and ($^1\text{A}_{1g} \rightarrow ^1\text{T}_{2g}$) corresponding with the octahedral geometry of these type complexes, the Pd^{II} complex shows the peaks at (668 nm) (14970 cm^{-1}) ($E_{\text{max}} = 152 \text{ Lcm}^{-1}\text{mol}^{-1}$) and (690 nm) (14492 cm^{-1}) ($E_{\text{max}} = 166 \text{ Lcm}^{-1}\text{mol}^{-1}$), referred to the d-d transition type ($^1\text{A}_{1g} \rightarrow ^1\text{B}_{1g}$) and ($^1\text{A}_{1g} \rightarrow ^1\text{B}_{2g}$) corresponding with the square planar geometry of these type complex²⁰⁻²¹.

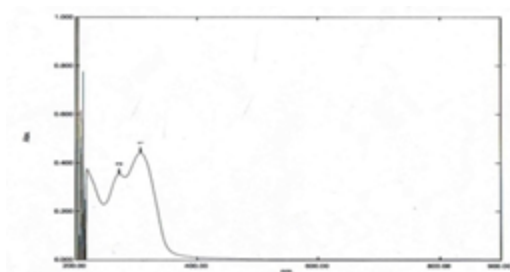


Figure (15) UV-Vis spectra of Ligand1

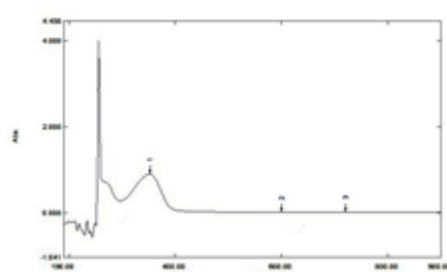


Figure (16) UV-Vis spectrum of Ligand1 with Ni^{II}

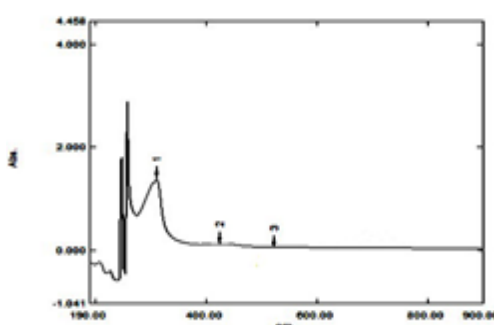
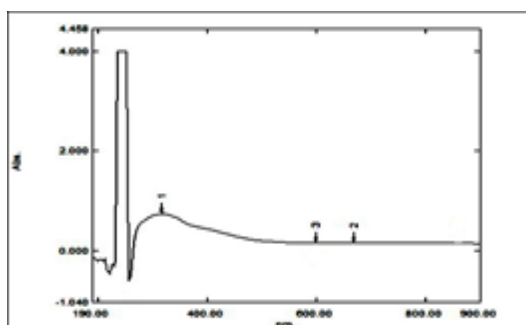


Figure (17) UV-Vis spectrum of Ligand1 with Pd^{II} Figure (18) UV-Vis spectrum of Ligand1 with Pt^{IV}

3:4:2-UV-Vis spectra of (L²) and their Complexes

The (UV-Vis) spectrum of [L²] **Fig.(19)** shows a broad absorption peak between (222- 334 nm) (45045 - 29940 cm⁻¹) (E_{\max} = 1255-1066 Lcm⁻¹mol⁻¹) due to ($\pi \rightarrow \pi^*$) transitions. The (UV-Vis) spectra for L² complexes with Ni^{II}, Pd^{II}, Pt^{IV} **Fig.(20)(21)(22)** respectively exhibits the absorptions at (344nm) (29069 cm⁻¹) (E_{\max} = 176 Lcm⁻¹mol⁻¹), (458 nm) (21834 cm⁻¹) (E_{\max} = 305 Lcm⁻¹mol⁻¹), and (328 nm) (30487cm⁻¹) (E_{\max} = 890 Lcm⁻¹mol⁻¹), respectively for Ni^{II}, Pd^{II}, Pt^{IV} ions attributed to the ligand field and charge transfer. The Ni complex shows the absorption at (708 nm)(14124 cm⁻¹) (E_{\max} = 169 Lcm⁻¹mol⁻¹), (788nm) (12690 cm⁻¹) (E_{\max} = 165 Lcm⁻¹mol⁻¹) and the Pt complex shows the absorption at (600nm) (16666 cm⁻¹) (E_{\max} = 85 Lcm⁻¹mol⁻¹) and (659nm) (15174 cm⁻¹) (E_{\max} = 74 Lcm⁻¹mol⁻¹) assigned to the d-d transition type ($^3A_{2g} \rightarrow ^3T_{1g}$) ($^3A_{2g} \rightarrow ^3T_{2g}$) for Ni^{II} and type ($^1A_{1g} \rightarrow ^1T_{1g}$) and ($^1A_{1g} \rightarrow ^1T_{2g}$) for Pt^{IV} complex, corresponding with the octahedral geometry of these type complexes, the Pd complex shows the absorption at (540nm) (18518 cm⁻¹) (E_{\max} = 307 Lcm⁻¹mol⁻¹) and (515nm) (16977 cm⁻¹) (E_{\max} = 310 Lcm⁻¹mol⁻¹) due to the d-d transition type ($^1A_{1g} \rightarrow ^1B_{1g}$) and ($^1A_{1g} \rightarrow ^1B_{2g}$) corresponding with the square planar geometry of these type complex²⁰⁻²¹.

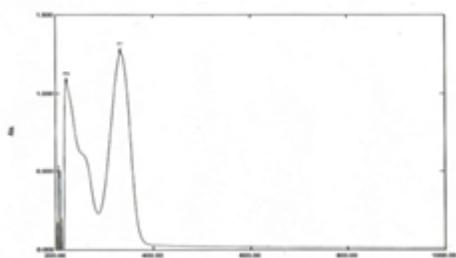


Figure (19) UV-Vis spectra of Ligand2

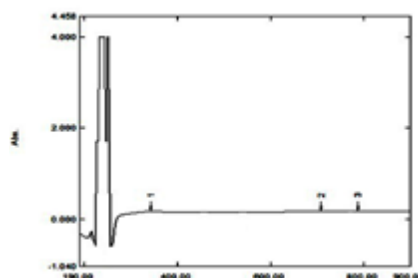


Figure (20) UV-Vis spectrum of Ligand2 with Ni^{II}

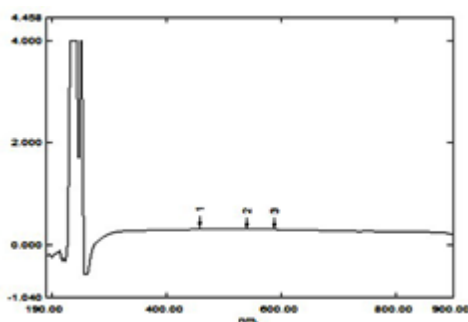


Figure (21) UV-Vis spectrum of Ligand2 with Pd^{II}

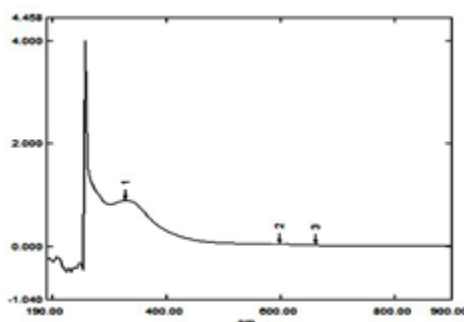


Figure (22) UV-Vis spectrum of Ligand 2 with Pt^{IV}

3:5-GC analysis

3:5:1-Gas chromatogram for L¹

The gas chromatogram shows **fig.(23)** for the (L¹) high purity appeared a peak at retention time (19.299).

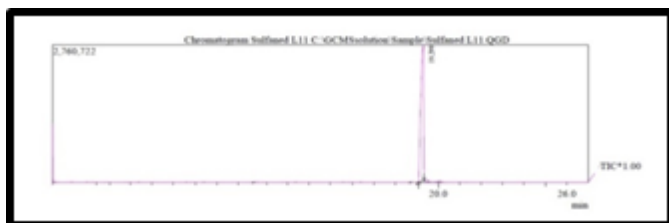


Figure (23)Gas chromatogram spectrum for Ligand 1

3:5:2-Gas chromatogram for L²

The gas chromatogram shows **fig.(24)** for the (L²) high purity appeared a peak at retention time (10.163).

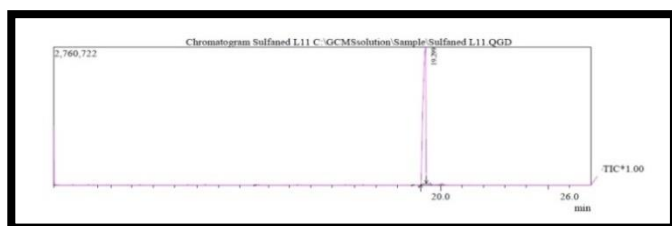


Figure (24)Gas chromatogram spectrum for Ligand 2

3:6-Conductivity measurements of complexes

The molar conductivity of complexes in DMSO solution in concentration (1×10^{-3} M) shows the nickel, palladium and platinum complexes is electrolyte in 1:4 ratio these results corresponding with results of magnetic susceptibility and electronic spectra data²². Shown **table (3)**.

3:7-Magnetic susceptibility of complexes

The magnetic susceptibility of the complexes appeared the prepared complexes were paramagnetic with (2.88 BM) for Ni²⁺ and diamagnetic (0.00 BM) for palladium and platinum. **Table (3)** summarized some physical properties of prepared complexes²³.

Table (3) Physical properties of synthesis complexes

No.	Complex	M.p. °C	Color	Yield %	Magnetic susceptibility B.M.	Conductivity Scm^2mol^{-1}	Suggested geometry
1	$[Ni_2(L^1)Cl_4]$	225- 227 Dec.	Pale green fine powder	61	2.45	17	Oh
2	$[Pd_2(L^1)]Cl_4$	161- 163 Dec.	Brown fine powder	56	0.00	170	Sp
3	$[Pt_2(L^1) Cl_4]$	245- 247	Black fine powder	46	0.00	173	Oh
4	$[Ni_2(L^2)Cl_4]$	174- 176	Green fine powder	65	2.67	18	Oh
5	$[Pd_2(L^2)]Cl_4$	167- 169 Dec.	Deep brown fine powder	68	0.00	185	Sp
6	$[Pt_2(L^2) Cl_4]$	270- 273	Orang fine powder	48	0.00	175	Oh

Dec.: decomposed, B.M.: Bohr magneton

3:8-Biological activity

As a result show in **Table (4)** of biological activity for ligands and their complexes series of different concentration 5 ppm, 10ppm and 15 ppm, in 5ppm have no biological activity for two ligands and their complexes and the best concentration was 15 ppm. The biological activity of ligands and their complexes against *E. coli* as a G-ve bacteria show the ligands have biological activity less than their complexes, the complexes of L2 have inhibition zoon best than L1 the highest inhibition zoon in L^2Pb (15ppm) (22mm). while found mild increase of biological activity in complexes of L1 against *Staph.aureus* as a G+ve bacteria but significant increase in biological activity of complexes of L2, the highest inhibition zoon in L^2Pt (15ppm) (22mm). This result because heavy metals conceder antimicrobial agent some metals work synergistically with antibiotic as a biocide use has been suggested as possible solution to antibiotic resistance. Heavy metal destroy bacterial cell by different ways like bind with vital cellular components such as structural protein, destroy functional enzyme by denaturation it, destroy nucleic acid and race oxidative stress that damage all biological macromolecules^{24,25}.

Table (4) Antibacterial activity for Ligands and their Metal complexes.

Compound	<i>Staphelococcus aurus</i>			<i>E.coli</i>		
	5mg	10mg	15mg	5mg	10mg	15mg
L^1	—	—	—	—	—	—
NiL^1	—	+	++	+	++	++
PdL^1	—	+	++	—	+	++
PtL^1	—	+	++	+	++	++
L^2	—	—	+	—	+	++
NiL^2	—	+	++	+	++	+++
PdL^2	—	++	+++	+	++	+++
PtL^2	—	++	+++	+	++	+++

ReferenceS

1. R.T.Morrison and R.N.Boyd, "Organic Chemistry", 6th Ed. Prentice Hall, New Delhi, India (2005).

2. J.K.Gupta, R.K.Yadav, R.Dudhe and P.K.Sharma, "Recent advancements in the synthesis and pharmacological evaluation of substituted 1, 3, 4-thiadiazole derivatives", *Int. J. PharmTech Res.*, (2010), 2(2):1493-1507
3. J.Goerdler, J.Ohm, and O.Tegmeyer, "Darstellung und Eigenschaften des 1.2.4- und des 1.3.4-Thiodiazols", *Chemische Berichte*, (1956), 89(6): 1534–1543
4. W.Samee and O.Vajragupta, "Antifungal, cytotoxic activities and docking studies of 2,5- dimercapto-1,3,4-thiadiazole derivatives", *African Journal of Pharmacy and Pharmacology*, 5, 4, 477-485 (2011).
5. J.Salimon, N.Salih, A.Hameed, H.Ibraheem and E.Yousif, "Synthesis and Antibacterial Activity of Some New 1,3,4-Oxadiazole and 1,3,4-Thiadiazole Derivatives", *Journal of Applied Sciences Research*, 6, 7, 866-870 (2010).
6. E.R.El-Sawy, M.S.Ebaid, H.M.Abo-Salem, A.G.Al-Sehemi and A.H.Mandour, "Synthesis, anti-inflammatory, analgesic and anticonvulsant activities of some new 4,6-dimethoxy-5- (heterocycles) benzofuran starting from naturally occurring visnagin", *Arab. J. Chem.*, 7, 6, 914–923 (2013).
7. Y.Chen, K.Yu, N.Y.Tan, R.H.Qiu, W. Liu, N.L.Luo, L.Tong, C.T.Au, Z.Q.Luo and S.F.Yin, "Synthesis, characterization and anti-proliferative activity of heterocyclic hypervalent organo antimony compounds", *Eur. J. Med. Chem.*, 79, 391–398, (2014).
8. F.Alam "A Study on the Antimicrobial and Antioxidant Activities of Some New 1, 3, 4-Thiadiazole Derivatives", *J. Chem. & Pharma. Res.*, 7, 5, 2520-2531 (2015).
9. M.S.Salem, S.I.Sakr, W.M.El-Senousy and H.M.F.Madkour, "Synthesis, antibacterial, and antiviral evaluation of new heterocycles containing the pyridine moiety", *Arch. Pharm. (Weinheim)*, 346, 10, 766–773 (2013).
10. C. L.praveena, V.E.Rani, and L.K .Ravindranath " Synthesis Characterization and Antimicrobial Activity of N- ((5-((6-OXIDO-6-(4 Substituted Phenoxy)-4,8-DIHYDRO-1H- [1,3,2] Dioxaphosphepino [5,6-C]Pyrazol-1-YL) Methyl)- 1,3,4-Thiadiazol-2-YL)Carbamoyl) Substituted Benzene Sulfonamides", *J. Chem. & Pharma. Res.*, 7, 01, 55-67 (2015).
11. S. Arunkumar "A Review on Synthetic Heterocyclic Compounds in Agricultural and other Applications", *J. Chem. & Pharma. Res.*, 8, 8, 170-179 (2015).
12. N.Kushwaha, S.K.S.Kushwaha, A.K.Rai "Biological Activities of Thiadiazole Derivatives: A Review", *J. Chem. & Pharma. Res.*, 4, 2, 517-531 (2012).
13. A.A.Hamid, H.J.Essa, A.H.Dawood "Synthesis, Characterization and Biological Activity Study of metronidazole- Thiadiazole derivatives", *J. Chem. & Pharma. Res.*, 9, 8, 428-438 (2016).
14. M.M.Saleh, S.F.AL-Joubori, and B.F.AL-Thamiar, "Synthesis and Antimicrobial Activity Of Some (2-Amino-5-Thiol-1,3,4-Thiadiazole Derivatives", *Um-Salama Science Journal*, 4, 1 (2007).
15. B.M.Suijkerbuijk, B.N.Aerts, H.P.Dijkstra, M.Lutz, A.L.Spek, G.van Koten and R. J. K.Gebbink, "“Click” 1, 2, 3-triazoles as tunable ligands for late transition metal complexes", *Dalton Transactions*, 13, 1273-1276 (2007).
16. A.H.AL-Daraji, "Synthesis and anti-microbial activity of transition metal complexes of 1,3,4-thiadiazole derivatives", *M.sc.Thesis*, Al-Nahrin university, Baghdad, Iraq (2000).
17. A.H.Dawood, E.T.Kareem and A.M.Madloul, "Binuclear Divalent Complexes of Cobalt, Nickel And Copper with N2S Ligand Derived from 1,3,4-thiadiazole 2,5-dithiolate Dipotassium Synthesized via Click Chemistry", *Inter. of Chem.*, 22, 1, 364-376 (2012).
18. C.Aswathanarayanappa, E.Bheemappa, Y.D.Bodke, S.Biradar, A.Sindhe, S.K.Peethambar, R.Ningegowda "Synthesis, invitro and invivo anti-hyperglycemic activity of 1,2,4-triazolebenzylidene and 1,3,4-thiadiazole derivatives", *J. Chem. & Pharma. Res.*, 6, 4, 1245-1255 (2014).
19. A.Thakur, P.R.S.Gupta, P.Pathak, A. Kumar "Design, Synthesis, SAR, Docking and antibacterial evaluation: Aliphatic amide bridged 4-aminoquinoline clubbed 1,2,4- triazole derivatives", *J. Chem. & Pharma. Res.*, 9, 03, 575-588 (2016).
20. A.H.Dawood, S.M.Hadawi and J.H.Abdol-Amer "synthesis and physical studies of mono and binuclear complexes with tetra and octa dentate ligands", *Inorg. Chem.*, 3, 69-72 (2012).
21. M.M.Abd-Elzaher, A.A.Labib, H.A.Mousa, W.A A.Mohamed, S.A.Moustafa "Synthesis, Spectral Structural Studies and 5 α -Reductase Inhibitory Activities of CoII, NiII, CuII, ZnII Mixed Ligand Complexes", *J. Chem. & Pharma. Res.*, 9, 08, 548-556 (2016).
22. S.A.Kettle "Coordination Compound", Thomas Nelson and Sons, London, pp.3, 186, 212 (1975).
23. M.A.Al-Soodani, "Synthesis and study of new 1,3,4-thiadiazole derivatives with some their Transition metal Complexes and identification their biological activity", *M.Sc.,Thesis*, Al-Mustansirya university, Baghdad, Iraq (2006).

24. K.J.Ryan, and C.G.Ray "Sherris Medical Microbiology", 4th Ed., McGraw-Hill Medical (2004).
25. H.G.Soğukömeroğulları, M.Sönmez, İ.Berber " Synthesis, characterization, antioxidant and antimicrobial studies of Cu(II), Co(II), Ni(II) and Mn(II) complexes with a new Schiff base ligand containing a pyrimidine moiety", J. Chem. & Pharma. Res., 9, 8, 391-398 (2016).
